Article

Cell Reports

DOC1-Dependent Recruitment of NURD Reveals Antagonism with SWI/SNF during Epithelial-Mesenchymal Transition in Oral Cancer Cells

Graphical Abstract

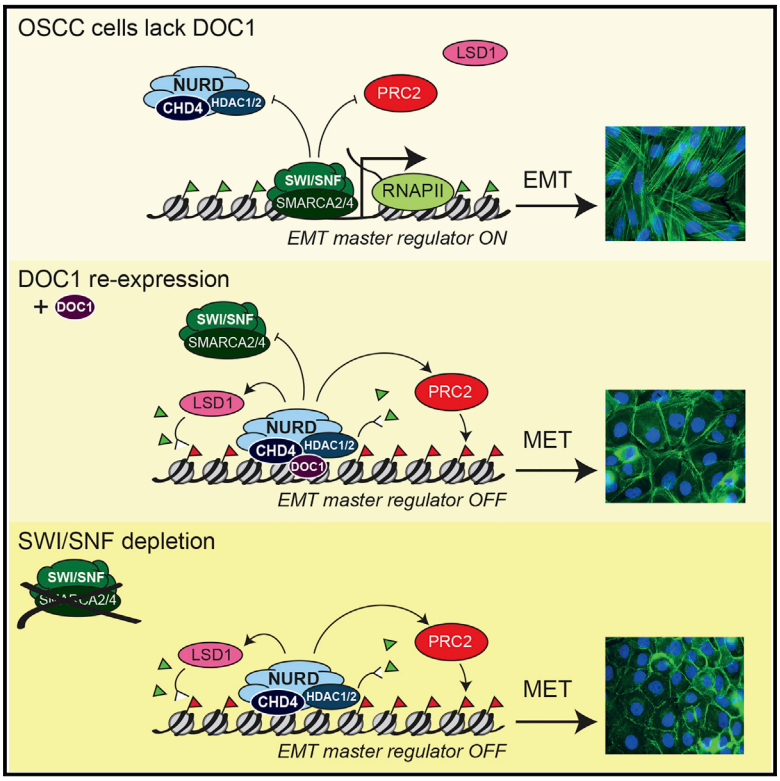

Highlights

- DOC1 re-expression in oral cancer cells causes a reversal of EMT
- DOC1 promotes NURD binding to a subset of target loci
- NURD and SWI/SNF compete for chromatin access, generating opposite epigenetic states
- Remodeler antagonism controls chromatin reprogramming of EMT

Authors

Adone Mohd-Sarip, Miriam Teeuwssen, Alice G. Bot, ..., Jeroen A. Demmers, Riccardo Fodde, C. Peter Verrijzer

Correspondence

a.mohdsarip@qub.ac.uk (A.M.-S.), c.verrijzer@erasmusmc.nl (C.P.V.)

In Brief

Mohd-Sarip et al. find that DOC1-dependent recruitment of NURD leads to reversal of the epithelial-mesenchymal transition (EMT) in oral cancer cells. Promoter binding of NURD drives SWI/SNF eviction, formation of repressive chromatin, and transcriptional repression of master regulators of EMT. The authors propose that remodeler antagonism controls reprogramming of EMT at the chromatin level.

Accession Numbers

GSE97839

Mohd-Sarip et al., 2017, Cell Reports *20*, 61–75
July 5, 2017
http://dx.doi.org/10.1016/j.celrep.2017.06.020

Cell Reports
Article

DOC1-Dependent Recruitment of NURD Reveals Antagonism with SWI/SNF during Epithelial-Mesenchymal Transition in Oral Cancer Cells

Adone Mohd-Sarip,[1,2,*] Miriam Teeuwssen,[3] Alice G. Bot,[2] Maria J. De Herdt,[4] Stefan M. Willems,[5] Robert J. Baatenburg de Jong,[4] Leendert H.J. Looijenga,[3] Diana Zatreanu,[2,10] Karel Bezstarosti,[6] Job van Riet,[7,8] Edwin Oole,[9] Wilfred F.J. van Ijcken,[9] Harmen J.G. van de Werken,[7,8] Jeroen A. Demmers,[6] Riccardo Fodde,[3] and C. Peter Verrijzer[2,11,*]

[1]Centre for Cancer Research and Cell Biology, Queen's University Belfast, Belfast BT9 7BL, UK
[2]Department of Biochemistry
[3]Department of Pathology
[4]Department of Otorhinolaryngology and Head and Neck Surgery, Erasmus MC Cancer Institute
Erasmus University Medical Center, P.O. Box 1738, 3000 DR, Rotterdam, the Netherlands
[5]Department of Pathology, University Medical Center Utrecht, Heidelberglaan 100, 3584 CX, Utrecht, the Netherlands
[6]Proteomics Centre
[7]Cancer Computational Biology Center, Erasmus MC Cancer Institute
[8]Department of Urology
[9]Center for Biomics
Erasmus University Medical Center, P.O. Box 1738, 3000 DR, Rotterdam, the Netherlands
[10]Present address: Mechanisms of Transcription Laboratory, The Francis Crick Institute, 1 Midland Road, L3-4384, London NW1 1AT, UK
[11]Lead Contact
*Correspondence: a.mohdsarip@qub.ac.uk (A.M.-S.), c.verrijzer@erasmusmc.nl (C.P.V.)
http://dx.doi.org/10.1016/j.celrep.2017.06.020

SUMMARY

The Nucleosome Remodeling and Deacetylase (NURD) complex is a key regulator of cell differentiation that has also been implicated in tumorigenesis. Loss of the NURD subunit Deleted in Oral Cancer 1 (DOC1) is associated with human oral squamous cell carcinomas (OSCCs). Here, we show that restoration of DOC1 expression in OSCC cells leads to a reversal of epithelial-mesenchymal transition (EMT). This is caused by the DOC1-dependent targeting of NURD to repress key transcriptional regulators of EMT. NURD recruitment drives extensive epigenetic reprogramming, including eviction of the SWI/SNF remodeler, formation of inaccessible chromatin, H3K27 deacetylation, and binding of PRC2 and KDM1A, followed by H3K27 methylation and H3K4 demethylation. Strikingly, depletion of SWI/SNF mimics the effects of DOC1 re-expression. Our results suggest that SWI/SNF and NURD function antagonistically to control chromatin state and transcription. We propose that disturbance of this dynamic equilibrium may lead to defects in gene expression that promote oncogenesis.

INTRODUCTION

ATP-dependent chromatin remodeling complexes (remodelers) control expression of the eukaryotic genome through the mobilization of nucleosomes. The nucleosome is the basic repeat unit of eukaryotic chromatin, comprising 147 bp of DNA, wrapped tightly around a protein core formed by an octamer of histones (Luger et al., 1997). Nucleosome positioning and stability determine the accessibility of regulatory DNA elements, thereby providing a pervasive mode of gene expression control. Consequently, remodelers play a central role in transcriptional regulation by mediating the assembly, sliding, restructuring, or ejection of nucleosomes (Becker and Workman, 2013; Narlikar et al., 2013). There are four major families of remodelers, each named after its ATPase subunit: SWI/SNF (Switch/Sucrose Non-fermentable), INO80, ISWI, and CHD. In addition to the central ATPase, remodeler complexes have unique sets of tightly associated proteins that determine targeting and regulate activity.

A second mechanism to control chromatin state involves a plethora of post-translational histone modifications, which can direct the recruitment of regulatory proteins (including remodelers) and modulate the folding of the chromatin fiber (Patel and Wang, 2013; Zentner and Henikoff, 2013). Prominent modifications include acetylation, methylation, and phosphorylation of specific residues on the histone N-terminal tails, which protrude from the nucleosome. There is a clear correlation between specific histone modifications and transcriptional state. For example, acetylation of histone H3K27 (H3K27ac) marks active genes, whereas tri-methylation of the same residue (H3K27me3) is associated with gene silencing by the Polycomb system. Although they mediate completely different biochemical reactions, remodelers and histone-modifying enzymes function in a closely integrated manner to determine chromatin state (Swygert and Peterson, 2014). In agreement with their central

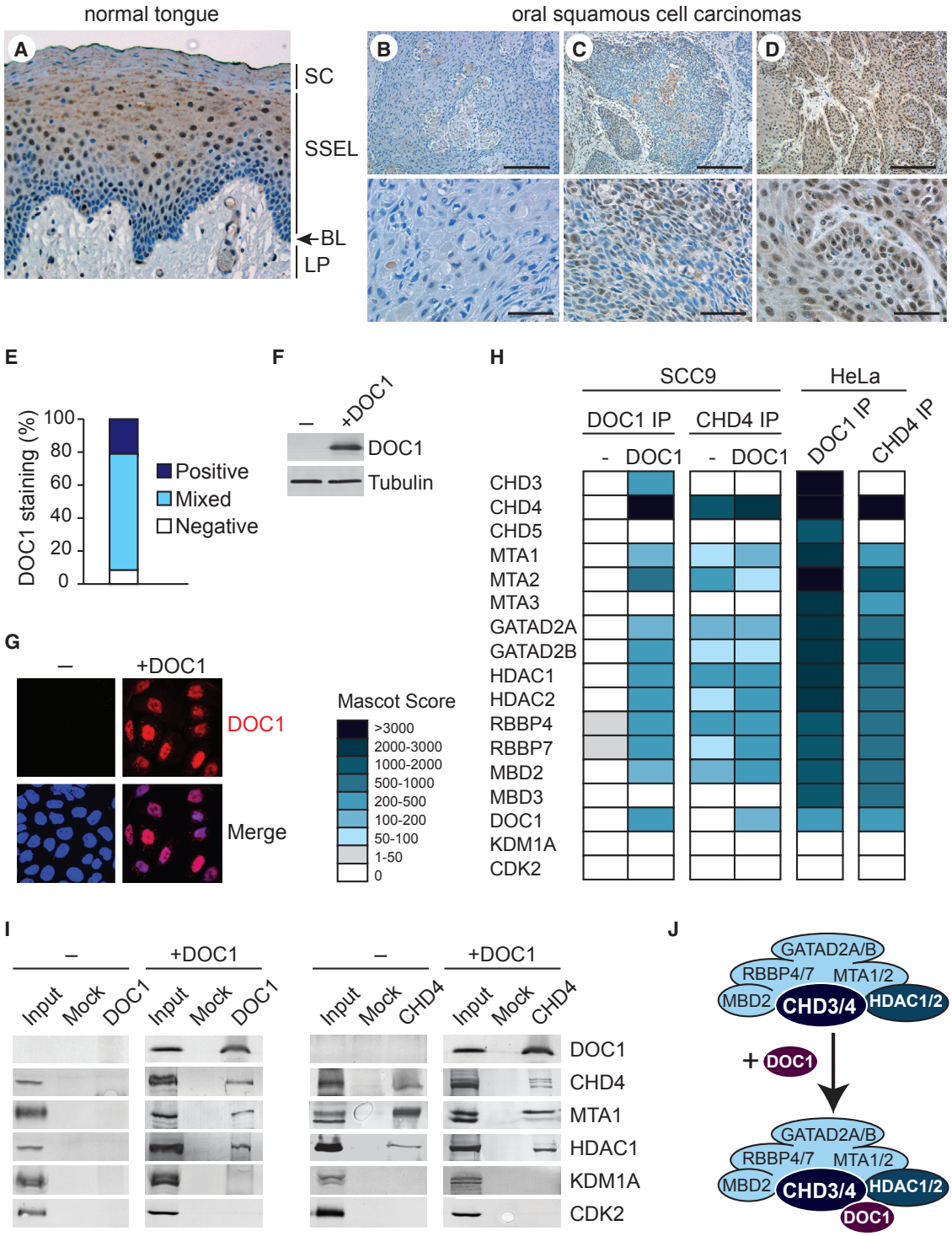

Figure 1. Re-expressed DOC1 in OSCC Cells Integrates into NURD

(A) Photomicrograph depicting DOC1 (brown), detected by immunohistochemistry, in a hematoxylin counterstained section of normal tongue epithelium. The underlying connective tissue of the lamina propria (LP), the BL, SSEL, and keratinized SC are indicated. Our anti-DOC1 antibodies strongly stain the nuclei of the SSEL.

(B–D) DOC1 expression in tongue carcinoma. Examples are of tumors that: (B) were negative for DOC1, (C) comprise a mixture of DOC1-negative and -positive cells, and (D) were strongly positive for DOC1. Scale bars, 200 μm (top row) or 50 μm (bottom row).

(E) Quantification of the DOC1 expression in 36 tongue carcinomas.

(legend continued on next page)

role in gene expression control, cancer genome sequencing studies have revealed frequent mutations in remodelers and histone-modifying enzymes across a broad spectrum of cancer types (Laugesen and Helin, 2014; Masliah-Planchon et al., 2015; Morgan and Shilatifard, 2015).

NURD refers to a family of protein assemblages that harbors one of the chromodomain ATP-dependent helicases CHD3, CHD4, and CHD5 (CHD3/4/5) and the histone deacetylases HDAC1 and HDAC2 (Torchy et al., 2015; Kolla et al., 2015). In addition to these two enzymatic activities, NURD comprises the scaffolding proteins GATAD2A/B, histone chaperones RBP4/7, histone tail- and DNA-binding proteins MTA1/2/3, and either one of the CpG-binding proteins MBD2 and MBD3. Notably, MBD2, but not MBD3, binds methylated CpG residues (Menafra and Stunnenberg, 2014). MBD2-NURD, rather than MBD3-NURD, has been implicated in the formation of repressive chromatin (Menafra and Stunnenberg, 2014; Günther et al., 2013). Finally, DOC1 (Deleted in Oral Cancer 1) is an initially overlooked, yet integral, subunit of NURD, conserved from *Drosophila* to humans (Reddy et al., 2010; Spruijt et al., 2010). DOC1 has also been identified as an interaction partner and negative regulator of CDK2, hence its alternate name: Cyclin-Dependent Kinase 2 Associated Protein 1 (CDK2AP1; Shintani et al., 2000; Wong et al., 2012). *Doc1* knockout mice are embryonic lethal at around day 3.5–5.5 days post-coitum (DPC) (Kim et al., 2009; Wong et al., 2012). Embryonic stem cells lacking *Doc1* self-renew but form exclusively mesodermal lineages in teratoma differentiation assays (Kim et al., 2009). NURD has been functionally connected to histone H3K27 methylation by Polycomb-Repressive Complex 2 (PRC2; Morey et al., 2008; Reynolds et al., 2012) and to H3K4me2 demethylation by KDM1A/LSD1 (Whyte et al., 2012; Laugesen and Helin, 2014). NURD plays essential roles in various developmental processes, as well as pluripotent stem cell differentiation, and has been implicated in oncogenesis (dos Santos et al., 2014; Hu and Wade, 2012; Lai and Wade, 2011; Laugesen and Helin, 2014; Signolet and Hendrich, 2015).

The gene encoding the 115-amino-acid (aa) DOC1 protein was first discovered as a potential tumor suppressor in oral cancer (Todd et al., 1995). Indeed, DOC1 is absent or downregulated in ~70% of human oral cancers (Shintani et al., 2001; Winter et al., 2011). Moreover, loss of DOC1 expression has also been observed in nasopharyngeal, gastric, and esophageal carcinomas (Choi et al., 2009; Hiyoshi et al., 2009; Wu et al., 2012). Pertinently, in these studies, low DOC1 expression correlated strongly with tumor invasion, metastasis, and adverse prognosis for patients. However, the molecular pathway through which loss of DOC1 promotes oncogenesis has remained unclear.

Epithelial-mesenchymal transition (EMT) is a reversible process that plays a central role in tumor malignancy (Puisieux et al., 2014; Ye and Weinberg, 2015). EMT is an integral part of normal development, allowing embryonic epithelial cells to become mobile and capable to colonize specific areas of the embryo. In cancer, however, EMT enables carcinoma cells to detach from the primary tumor, invade surrounding tissue, and disseminate to distant sites to form metastases. EMT is orchestrated by a transcriptional program directed by a small set of evolutionary conserved master transcription factors, including TWIST, SNAIL, ZEB, and SLUG (Puisieux et al., 2014). EMT transcription factors exert additional oncogenic activities, e.g., escape from senescence or apoptosis, adoption of stem-cell-like properties, and drug resistance, even in cancer cells retaining epithelial features.

Here, we investigated the molecular function of DOC1 in oral cancer. We found that tumor suppression by DOC1 involves the reversal of EMT, which is caused by NURD-dependent repression of EMT transcription factors. DOC1 mediates the recruitment of NURD, initiating comprehensive epigenetic reprogramming and transcriptional silencing. Our results reveal that NURD and SWI/SNF function antagonistically to control gene expression, through modulation of nucleosome remodeling and Polycomb recruitment.

RESULTS

Loss of the NURD Subunit DOC1 in Oral Cancer Cells

Similar to the better studied SWI/SNF remodelers, the sequencing of cancer genomes has uncovered frequent mutations in genes encoding NURD subunits (Figure S1A; http://www.cbioportal.org). These observations suggest that inactivation of NURD might contribute to oncogenesis. Although rarely mutated in most cancer types, DOC1 levels are reduced in the majority of human oral cancers, and the loss of DOC1 correlates with tumor invasion and metastasis (Shintani et al., 2001; Winter et al., 2011). Prompted by these findings, we examined DOC1 expression in normal and cancerous tongue tissue (Figures 1A–1E). Immunohistochemistry (IHC) of normal tongue tissue suggests a relationship between DOC1 expression and epithelial cell differentiation (Figure 1A). DOC1 is mostly undetectable in the basal layer (BL) where the epithelial stem cells reside. However, DOC1 is induced during cell differentiation and is robustly expressed in nuclei within the stratified squamous epithelial layer

(F) Immunoblotting analysis of DOC1 expression in SCC9 cells transduced with lentiviruses expressing either an irrelevant control (LacZ, indicated with a minus symbol) or DOC1. Tubulin serves as a loading control.
(G) Indirect IF of SCC9 cells treated as described above. Cells were fixed and stained with antibodies against DOC1 (red). Nuclei were visualized by DAPI staining of DNA (blue). See Figures S1B and S1C for additional OSCC cell lines.
(H) Interaction heatmap, based on mascot scores, depicting associated factors identified by mass spectrometry after IP of DOC1 or CHD4 from SCC9 cells transduced with lentiviruses expressing either an irrelevant control (LacZ, indicated with a minus symbol) or DOC1. In addition, endogenous DOC1 and CHD4 were immunopurified from HeLa cells. See Table S1 for details and IPs from SCC4 cells.
(I) Co-IPs of DOC1 or CHD4 from SCC9 cells. Associated proteins were detected by immunoblotting with antibodies against the indicated proteins. Input represents 10% of the binding reactions. See Figure S1D for co-IPs from HeLa cells.
(J) Cartoon summarizing the proteomics results.
See also Figure S1 and Table S1.

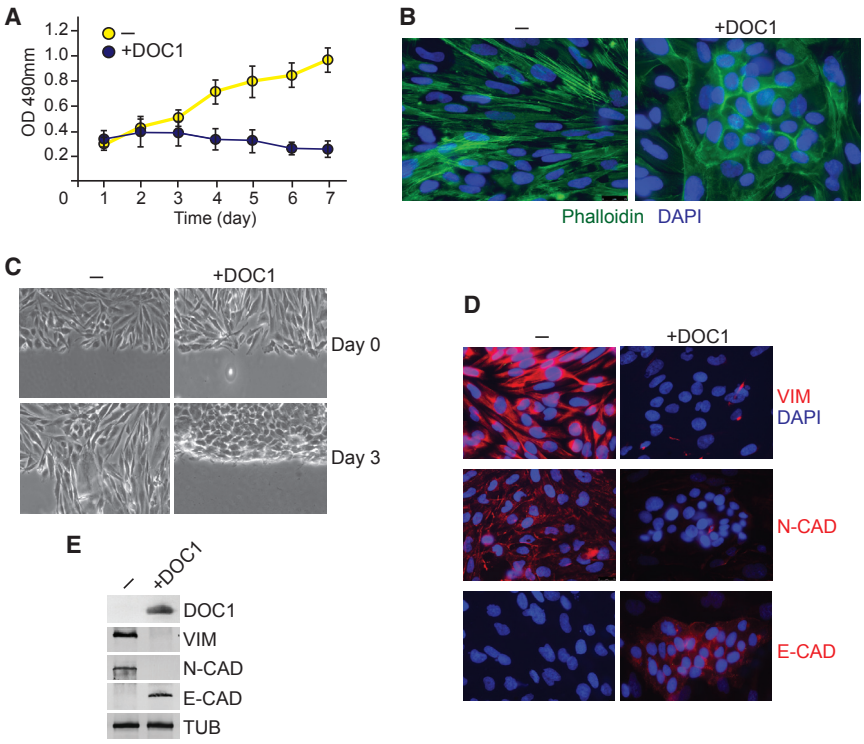

Figure 2. DOC1 Expression Causes MET in OSCC Cells

(A) Re-expression of DOC1 attenuates cell proliferation. Proliferation curves of SCC9 cells transduced with lentiviruses expressing either LacZ (yellow graph) or DOC1 (blue graph), as determined by the Aqueous One Proliferation Assay (Promega). Means and SEMs were derived from three independent biological replicates. See Figure S2A for cell-cycle analysis and Figures S2B–S2D for additional OSCC cell lines. OD 490nm, optical density at 490 nm.

(B) DOC1 affects cell shape and actin organization in OSCC cells. Indirect IF of SCC9 cells that either lack (–) or express DOC1. F-actin was visualized by phalloidin staining (green), and nuclei were visualized by DAPI staining of DNA (blue). See Figure S2E for other OSCC cell lines.

(C) DOC1 inhibits migration of SCC9 cells. The effect of DOC1 on migratory behavior of SCC9 cells was tested by a wound healing assay. Light microscopic images were taken directly following scratching a monolayer of cells (day 0) and 3 days later.

(D) DOC1 induces MET in OSCC cells. Indirect IF of SCC9 cells stained (red) with antibodies against VIM, N-CAD, and E-CAD. Nuclei were visualized by DAPI staining of DNA (blue). See Figure S2E for other OSCC cell lines.

(E) Immunoblotting analysis of the effect of DOC1 on expression of EMT markers. Tubulin (TUB) serves as a loading control.

See also Figure S2.

(SSEL). However, when the keratinocytes undergo terminal differentiation and cornification within the stratum corneum (SC), DOC1 levels are reduced again. Analysis of a cohort of 36 human oral squamous cell carcinomas (OSCCs) of the tongue revealed a small percentage (~8%) that were completely negative for DOC1 (Figure 1B), whereas the majority showed a mixture of negative and positive cells (Figure 1C), and ~20% were positive (Figures 1D and 1E). Moreover, we found that DOC1 was lacking in all four different human OSCC cell lines that we examined (SCC4, SCC9, SCC15, and SCC25), while it was readily detected in HaCaT keratinocytes (Figures 1F, 1G, S1B, and S1C). Thus, in agreement with previous studies, we observed reduced DOC1 expression in the majority of OSCCs.

To study its role in OSCC cells, we re-expressed *DOC1* by lentiviral transduction (Figures 1F, 1G, and S1B). Next, we immunopurified DOC1 from whole-cell extracts (WCEs) prepared from SCC9 cells transduced with either LacZ- or DOC1-expressing virus. Mass spectrometric analysis revealed the association of DOC1 with CHD3, CHD4, MTA1, MTA2, GATA2A, GATA2B, HDAC1, HDAC2, RBBP4, RBBP7, and MBD2 (Figure 1H; Table S1). Purification of CHD4 revealed a similar complex but lacking CHD3. CHD5, MTA3, and MBD3 were absent in the immunoprecipitations (IPs) from SCC9 cells. The presence or absence of DOC1 did not substantially affect the composition of the NURD complex, although there were subtle changes in the mass spectrometric scores for specific subunits. Thus, DOC1 does not appear to play a major architectural role in the NURD complex. IPs of DOC1 and CHD4 from SCC4 cells yielded similar results (Table S1). Mass spectrometric analysis of endogenous DOC1 immunopurified from HeLa cells revealed the full complement of NURD-class proteins, including CHD3/4/5, MBD2/3, and MTA1/2/3 (Figure 1H; Table S1). CHD4 immunopurified from HeLa cells was associated with a similar set of proteins, but CHD3 and CHD5 were absent. Immunoblotting of DOC1- and CHD4-bound proteins confirmed the mass spectrometric results (Figures 1I and S1D). Under the conditions used (buffers including 600 mM KCl and 0.1% NP-40), CDK2 was not present in our DOC1 IPs. Likewise, we did not detect the association of KDM1A with NURD, which has been debated in the literature (Laugesen and Helin, 2014). We conclude that DOC1 is an integral subunit of the MBD2/3/CHD3/4/5-NURD family of complexes. OSCC cells lack DOC1, but when re-expressed, DOC1 integrates into NURD (Figure 1J). Next, we examined the effects of DOC1 re-expression in OSCC cells.

DOC1 Attenuates OSCC Cell Proliferation and Induces MET

DOC1 expression in SCC9 cells causes a marked attenuation of cell proliferation (Figure 2A; throughout this paper, yellow graphs refer to mock-treated cells, and blue graphs refer to OSCC cells expressing DOC1). We did not observe an arrest at a defined stage of the cell cycle, increased apoptosis, or cellular senescence (Figure S2A). Most likely, this is due to the inactivation of the p53 and p16INK4a tumor suppressor pathways in these OSCC cells (http://www.lgcstandards-atcc.org). DOC1 also inhibited proliferation of the other OSCC cell lines (SCC4,

SCC15, and SSC25; Figures S2B–S2D). Surprisingly, DOC1 re-expression induced marked changes in SCC9 cell morphology and actin organization, as visualized by phalloidin staining (Figure 2B). Compared to cells transduced with a control vector, which have a more fibroblast-like appearance, DOC1-expressing cells acquire a more cobblestone-like morphology with epithelial features. Moreover, upon DOC1 expression, prominent stress fibers are replaced by a more cortical actin organization. A scratch test revealed that DOC1-expressing SCC9 cells are less migratory and form layers of tightly attached cells (Figure 2C). These results suggest that expression of DOC1 induces a mesenchymal-to-epithelial transition (MET). To test this possibility, we examined the expression of a number of canonical EMT markers. Immunofluorescence (IF) microscopy revealed a strong reduction of the mesenchymal markers vimentin (VIM) and N-cadherin (N-CAD) after DOC1 expression, whereas the epithelial marker E-cadherin (E-CAD) was upregulated (Figures 2D and S2E). The observed changes in expression of these EMT markers were confirmed by immunoblotting (Figure 2E).

In conclusion, we examined the effects of DOC1 re-expression in OSCC cells that lack this integral subunit of NURD. DOC1 efficiently incorporates into NURD and triggers the differentiation of cells from a quasi-mesenchymal (SCC9 and SCC15) or quasi-epithelial (SCC4 and SCC25) appearance toward an epithelial phenotype. Therefore, DOC1-induced cell differentiation is, strictly speaking, a partial MET. For the sake of brevity, however, we will, hereinafter, refer to this process as MET. This transition involves changes in actin organization, cell shape, expression of key EMT markers, reduced cell migration, and attenuated cell proliferation. These observations suggest that loss of DOC1 contributes to the development of OSCC by inhibiting epithelial differentiation and by conferring tumor cells with a mesenchymal-like and, possibly, more invasive phenotype.

DOC1 Functions as Part of NURD

To test whether the effects of DOC1 re-expression in OSCC cells depend on the chromatin remodeling activity of the NURD complex, we depleted its ATPase CHD4 (Figure 3A). Following short hairpin RNA (shRNA)-mediated knockdown of CHD4 in SCC9 cells, DOC1 expression failed to trigger MET. There was no induction of E-CAD, whereas VIM and N-CAD expression was not reduced. Loss of CHD4, in the absence of DOC1 expression, did not affect the expression of EMT markers. Regardless of the presence or absence of DOC1, knockdown of CHD4 led to reduced cell proliferation (Figure 3B). Likewise, depletion of MBD2 or MTA2 caused a loss of cell viability and blocked the ability of DOC1 to promote MET (Figures S3A and S3B). Thus, once NURD lacks DOC1, loss of additional NURD subunits compromises cell viability but has little effect on the expression of EMT markers. Thus, the capacity of DOC1 to drive MET depends on NURD, and cells lacking DOC1 still depend on the remaining NURD for viability.

Next, we used shRNAs to deplete either DOC1, CHD4, MBD2, or MTA2 in HaCaT cells, a spontaneously immortalized, human keratinocyte line (Figures 3C, 3D, and S3C–S3E). Under our culture conditions, HaCaT cells have an epithelial phenotype. Upon knockdown of DOC1 or other NURD subunits, there was reduced expression of the epithelial marker E-CAD, whereas the mesenchymal markers N-CAD and VIM were induced (Figures 3C and S3C). In agreement with our earlier results (Figure 1J), loss of DOC1 did not affect the stability of other NURD subunits (Figure S3D). However, loss of MBD2 or MTA2 affected CHD4 levels, suggesting that these subunits are important for the structural integrity of NURD. Importantly, depletion of either DOC1, CHD4, MBD2, or MTA2 caused substantially reduced cell numbers (Figures 3D and S3E). Thus, the intact NURD complex is required for optimal viability of HaCaT cells. Collectively, these observations support the notion that DOC1 functions as an integral part of NURD.

DOC1-Dependent Recruitment of NURD Drives MET

The EMT program is orchestrated by a set of master regulators that form an integrated transcriptional network with extensive cross-regulation. Expression of DOC1 in OSCC cells leads to downregulation of all major EMT transcription factors, concomitant with cell differentiation toward an epithelial phenotype (Figure 4A). To determine which of these might be directly regulated by NURD, we used chromatin IP (ChIP)-qPCR. We monitored CHD4 binding to selected promoter regions in either the absence or presence of DOC1. CHD4 ChIPs revealed strong DOC1-dependent binding to the promoters of *Twist1*, *Twist2*, and *Zeb2* and weaker binding to the *Snail*, *Slug*, and *Zeb1* promoters (Figure 4B). CHD4 binding to two previously identified targets of NURD, *Crabp1* and *Rassf10* (Günther et al., 2013), was independent of DOC1. The binding pattern of DOC1 was similar to that of CHD4 (Figure 4C). Collectively, these results suggest that DOC1 is a gene-selective subunit of NURD, required for the binding and repression of key EMT transcription factor genes.

NURD-mediated repression of crucial master regulators of EMT provides an attractive molecular mechanism to explain DOC1-induced MET in OSCC cells. To test this hypothesis, we transduced lentiviruses that expressed shRNAs directed against either *Twist1* or *Twist2* or a control virus (mock). Depletion of either TWIST1 or TWIST2, in the absence of DOC1 expression, suffices to induce MET, as indicated by actin reorganization, downregulation of VIM and N-CAD, and induction of E-CAD (Figures 4D and 4E). TWIST1 and TWIST2 appear both to be required for EMT. As observed for DOC1 re-expression in OSCC cells, loss of TWIST1/2 inhibited cell proliferation (Figure 4F). These results establish that downregulation of TWIST1 or TWIST2 can mimic the main effects of DOC1 re-expression in OSCC cells. These results suggest that DOC1 initiates MET in oral cancer cells by directing NURD to repress master regulators of EMT.

NURD Recruitment Causes Extensive Chromatin Reorganization

To explore the impact of NURD recruitment on the local chromatin structure, we first determined its precise localization within ~900 bp of the *Twist1* promoter region (−500 to +400 bp, relative to the transcription start site; TSS). ChIP-qPCR revealed DOC1-dependent CHD4 binding, directly upstream of the *Twist1* transcription start site (Figure 5A). Histone H3 ChIPs revealed a prominent nucleosome-depleted region (NDR) in the absence of DOC1 when *Twist1* is expressed (Figure 5B). Following DOC1 expression and NURD binding, there is a dramatic nucleosome repositioning, leading to occupancy of the NDR.

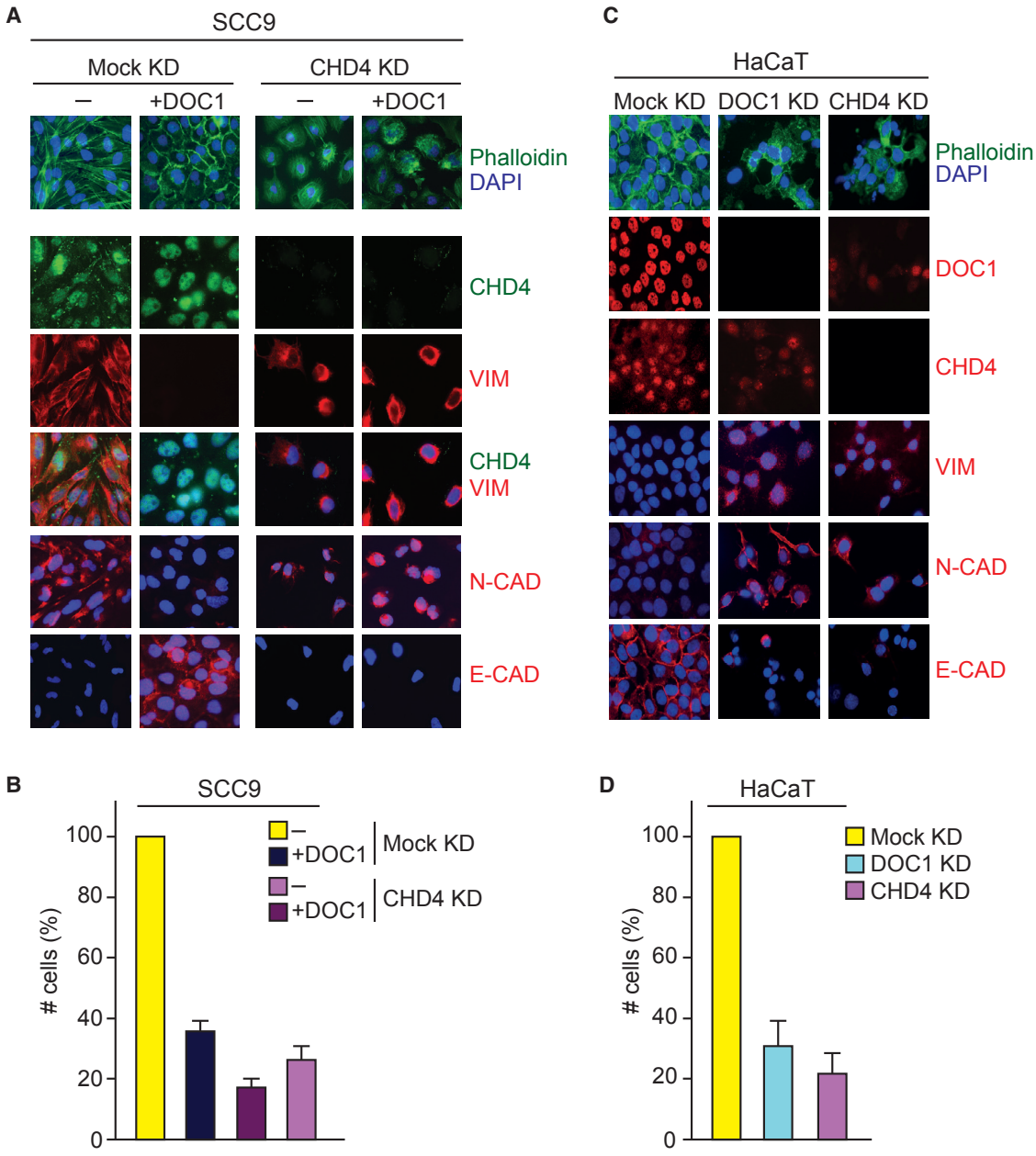

Figure 3. DOC1-Induced MET Depends on CHD4

(A) Indirect IF of SCC9 cells that either lack or express DOC1, in combination with shRNA-mediated knockdown (KD) of CHD4. Cells were stained using the indicated antibodies.

(B) Effects of DOC1 expression in combination with CHD4 KD on cell proliferation were determined 3 days after KD, as described in the legend for Figure 2A.

(C) Indirect IF of HaCaT cells after KD of DOC1 or CHD4. Cells were stained using the indicated antibodies.

(D) HaCaT cell numbers were determined 3 days following KD of DOC1 or CHD4.

Means and SEMs were derived from three independent biological replicates.

See also Figure S3.

High-resolution micrococcal nuclease (MNase) sensitivity mapping showed that, in the absence of DOC1, the *Twist1* promoter DNA was highly accessible to nuclease digestion (Figure 5C). In addition, MNase mapping established that the ~250-bp NDR is flanked by well-positioned nucleosomes. DOC1 expression induces extensive chromatin reorganization, leading to complete occlusion of the NDR and a shift in the position of the flanking nucleosomes. Thus, DOC1-mediated recruitment of NURD to the *Twist1* promoter induces a switch from an open to closed nucleosomal organization.

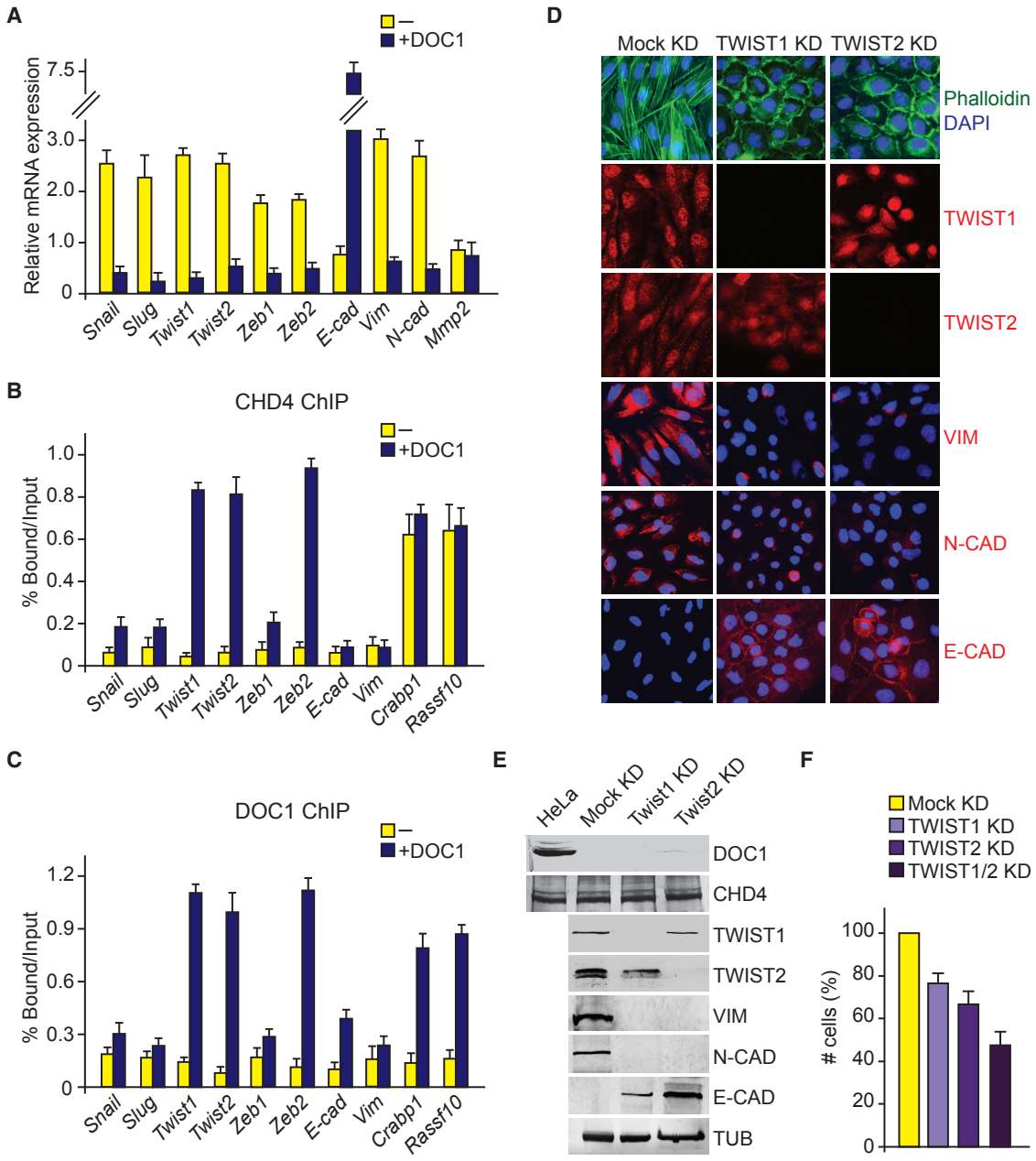

Figure 4. DOC1-Mediated Repression of *TWIST1/2* Drives MET

(A) Effect of DOC1 on the expression of EMT transcription factors. mRNA was isolated from SCC9 cells that either lacked (yellow bars) or expressed (blue bars) DOC1. Relative levels of mRNA were determined by qRT-PCR. *Gapdh* was used for normalization. Means and SDs were derived from three independent biological replicates.

(B) DOC1 is required for CHD4 binding to the *Twist1*, *Twist2*, and *Zeb2* promoters. ChIP-qPCR analysis of DOC1 binding to the promoters of EMT transcription factors, *E-cadherin*, *Vimentin*, *Crabp1*, and *Rassf10*. Chromatin was isolated from SCC9 cells that either lacked (yellow bars) or expressed DOC1 (blue bars). Means and SDs were derived from three independent biological replicates.

(C) ChIP-qPCR analysis of DOC1 binding. Means and SEM were derived from three independent biological replicates.

(D) Depletion of TWIST1 or TWIST2 suffices for MET. Indirect IF of SCC9 cells after knockdown (KD) of either TWIST1 or TWIST2. Cells were stained with phalloidin or the indicated antibodies.

(E) Immunoblotting analysis of the effect of DOC1 on the expression of EMT markers, using antibodies against the indicated proteins.

(F) Effect of KD of TWIST1 or TWIST2 on cell proliferation were determined 3 days after KD, as described in the legend to Figure 2A. Means and SEMs were derived from three independent biological replicates.

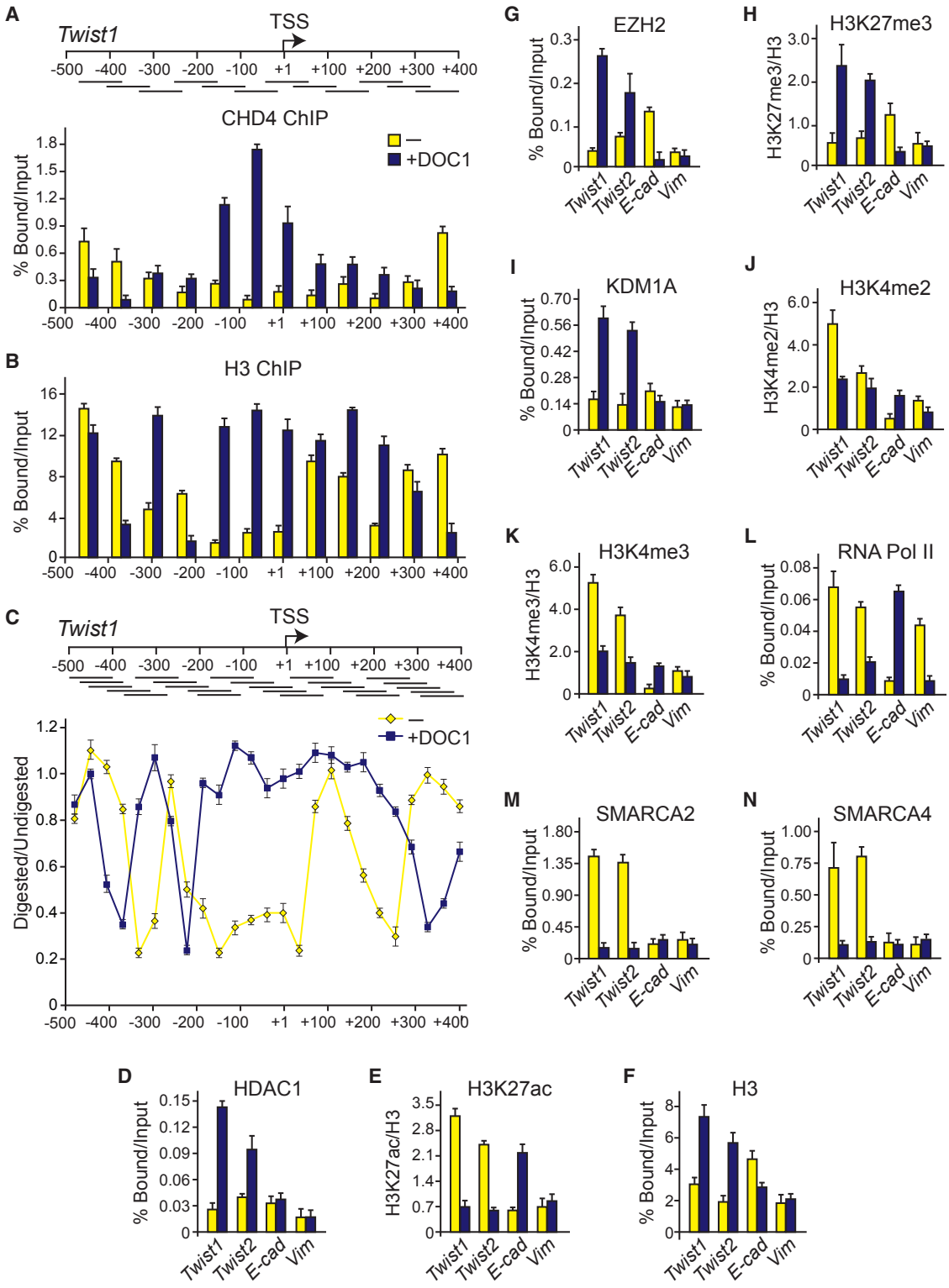

Figure 5. DOC1 Directs Epigenetic Reprogramming of *Twist1/2*

(A) DOC1-dependent binding of CHD4 to the *Twist1* promoter region. ChIP-qPCR analysis of CHD4 binding to chromatin isolated from SCC9 cells that either lacked (yellow bars) or expressed (blue bars) DOC1. The diagram depicts the PCR amplicons used covering positions −480 to +400 of the *Twist1* gene. The transcription start site (TSS) is +1.

(B) Histone H3 ChIP-qPCR.

(legend continued on next page)

In addition to nucleosome remodeling, NURD mediates histone deacetylation. As expected, HDAC1 was readily recruited to the *Twist1* and *Twist2* promoters following DOC1 expression (Figure 5D). Concomitantly, there was a drop in the level of H3K27 acetylation, corrected for histone H3 occupancy (Figure 5E). Similar to the *Twist1* promoter, histone H3 ChIP revealed DOC1-induced nucleosome occupancy at the *Twist2* promoter (Figure 5F). H3K27 deacetylation by NURD has been linked to the recruitment of PRC2 (Reynolds et al., 2012). Indeed, in the presence of DOC1, we observed binding of the PRC2 enzymatic subunit EZH2, accompanied by increased levels of H3K27me3 (Figures 5G and 5H). Moreover, DOC1 expression was followed by binding of the KDM1A, with concomitant loss of H3K4me2 and H3K4me3 (Figures 5I and 5K). The transfer from an active to a repressed chromatin state was accompanied by loss of RNA polymerase II (RNA Pol II; Figure 5L). Similar to what we observed for the *Twist1/2* promoters, DOC1-dependent binding of NURD to the promoter region of *Zeb2* induced formation of a repressive chromatin structure (Figures S4A–S4K). Thus, NURD recruitment initiates the comprehensive epigenetic reprogramming of the *Twist1/2* and *Zeb2* genes.

Previously, we reported that the SWI/SNF remodeler counteracts chromatin binding of Polycomb repressors (Kia et al., 2008). Therefore, we wondered whether SWI/SNF might be associated with the active *Twist1/2* and *Zeb2* promoters to prevent Polycomb repression. We performed ChIP assays using antibodies directed against either SMARCA4/BRG1 or SMARCA2/hBRM, the mutually exclusive ATPase subunits of SWI/SNF assemblages. Both SMARCA2 and SMARCA4 bound the active *Twist1/2* and *Zeb2* promoters but were displaced following DOC1-driven binding of NURD (Figures 5M, 5N, and S4L–S4N). These observations raised the possibility that SWI/SNF and NURD act antagonistically in the control of the *Twist1/2* and *Zeb2* genes.

Loss of SWI/SNF Phenocopies the Effects of DOC1 Re-expression

To test the idea that SWI/SNF and NURD might have opposing effects on the EMT program, we determined the consequences of SWI/SNF depletion in the absence of DOC1 induction. Depletion of either SMARCA2 or SMARCA4 had only weak effects on SCC9 cell phenotype (Figure S5A). However, knockdown of both SWI/SNF ATPases induced a strong MET. Loss of both SMARCA2 and SMARCA4 (SMARCA2/4) led to actin fiber re-organization and a change from a fibroblast-like morphology to an epithelial cell shape (Figure 6A). We observed the downregulation of VIM and N-CAD, whereas E-CAD was induced (Figures 6B and S5B). Moreover, there was a loss of *Twist1/2* and *Zeb2* expression after SMARCA2/4 depletion (Figure 6C; yellow indicates mock, and red indicates SMARCA2/4 knockdown). Loss of either SMARCA2 or SMARCA4 alone gave an intermediate effect, suggesting that both remodelers stimulate *Twist1/2* and *Zeb2* transcription (Figure S5C). Finally, depletion of SMARCA2/4 led to diminished cell numbers (Figure S5D). Thus, the functional consequences of SWI/SNF depletion are similar to those of DOC1 re-expression: reduced cell proliferation, attenuated expression of EMT transcription factors, and MET. Our results suggest that SWI/SNF and NURD compete for chromatin binding at *Twist1/2* and *Zeb2* promoters and generate opposite transcriptional states. To test this idea, we examined the impact of SWI/SNF depletion on chromatin organization.

Remodeler Antagonism Controls Epigenetic Reprogramming of EMT

Both SMARCA2 and SMARCA4 bind to the *Twist1/2* and *Zeb2* promoters (Figures 6D, 6E, S6B, and S6C). Knockdown of SMARCA2/4 caused a loss of ChIP signals, confirming the specificity of our antibodies. Following SWI/SNF depletion, the NDR disappears and the *Twist1* promoter DNA is now occluded by nucleosomes (Figures 6F and S5E). The pattern of MNase accessibility after the knockdown of SWI/SNF is remarkably similar to that following DOC1 expression (compare Figures 5C and 6F). CHD4 and HDAC1 ChIPs showed that depletion of SWI/SNF suffices to allow NURD binding to the *Twist1/2* and *Zeb2* promoters, in spite of the absence of DOC1 (Figures 6G, S5F, S6D, and S6E). These results show that NURD devoid of DOC1 still has an intrinsic, albeit weakened, ability to bind the *Twist1/2* and *Zeb2* promoters. The chromatin changes caused by SWI/SNF depletion are remarkably similar to those observed after DOC1 re-expression (Figures 6H–6J, S5G–S5K, and S6F–S6M). Concomitant with NURD recruitment after SWI/SNF knockdown, the level of H3K27ac dropped, PRC2 bound, and H3K27ac was replaced by H3K27me3. In addition, KDM1A is recruited, accompanied by H3K4 demethylation. In agreement with the repression of *Twist1/2* and *Zeb2* transcription, RNA Pol II is lost following the knockdown of SWI/SNF. Thus, SWI/SNF depletion in OSCC cells has similar effects on the epigenetic setting of EMT master regulators as DOC1 re-expression.

In summary, SWI/SNF prevents the binding of NURD lacking DOC1 to the *Twist1/2* and *Zeb2* promoters. Conversely, upon inclusion of DOC1 in the complex, NURD displaces SWI/SNF. The replacement of SWI/SNF by NURD results in the transition from an open to a closed chromatin structure. Moreover, chromatin binding by PRC2 is blocked by SWI/SNF but promoted by NURD. Thus, SWI/SNF and NURD compete for binding and

(C) DOC1-induced changes in nucleosome organization. High-resolution MNase accessibility mapping on chromatin isolated from cells that either lacked (yellow graph) or expressed (blue graph) DOC1. The MNase accessibility profile was determined by normalizing the amount of digested PCR product to that of the undigested product using the delta C(t) method. Ratios were plotted against the midpoint of the corresponding PCR amplicons shown in the diagram on top.
(D–N) ChIP-qPCR analysis of chromatin at the Twist1, Twist2, E-cadherin, and Vimentin promoters using antibodies directed against (D) HDAC1, (E) H3K27ac, (F) H3, (G) EZH2, (H) H3K27me3, (I) KDM1A, (J) H3K4me2, (K) H3K4me3, (L) RNA PolII, (M) SMARCA2, and (N) SMARCA4. Chromatin was isolated from SCC9 cells that either lacked (yellow bars) or expressed DOC1 (blue bars). Protein ChIP signals are presented as percentage of input chromatin. Histone modification ChIPs were normalized to H3 signals.
Means and SEMs for all experiments in this figure were derived from three independent biological replicates. Results for the *Zeb2* promoter are shown in Figure S4.
See also Figure S4.

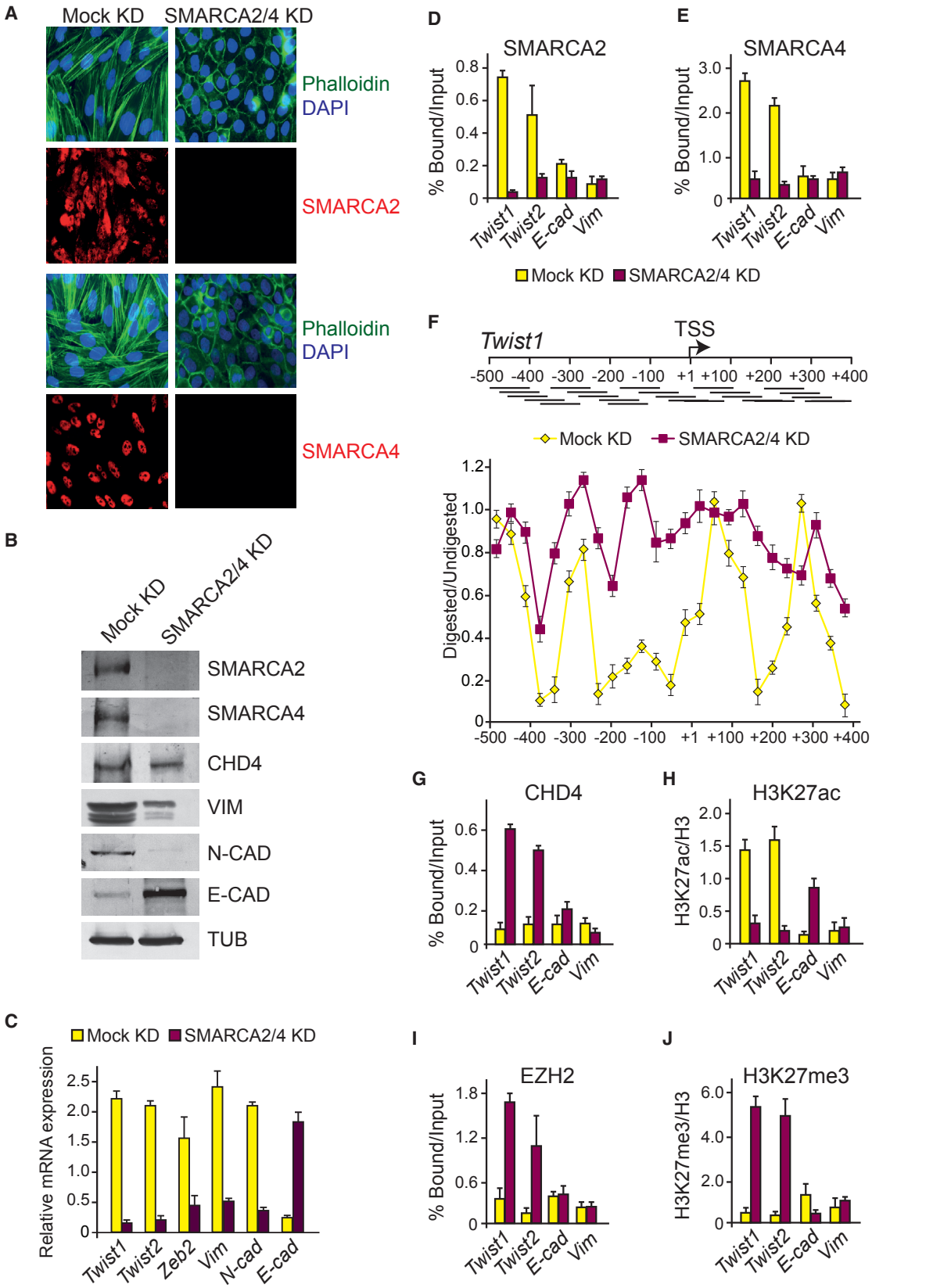

(legend on next page)

generate opposite chromatin states. We propose that a disturbance in the balance between these antagonistic remodelers can set off a cascade of chromatin reprograming that promotes oncogenesis.

DOC1 Assists NURD Recruitment to CpG Islands

To investigate the impact of DOC1 on the genome-wide binding of NURD, we performed CHD4 ChIP sequencing (ChIP-seq) on chromatin from SCC9 cells. We identified 4,902 CHD4 consensus peaks in DOC1-expressing cells, compared to 3,949 in cells lacking DOC1. This observation indicates that DOC1 is important for binding to a subset of NURD loci. We note that the ChIP-seq uncovered DOC1-dependent binding to additional genes involved in EMT, as illustrated with a few examples in Figure 7A. Analysis of the genomic distribution of CHD4 revealed that about 60% (no DOC1) to 67% (+DOC1) of the binding sites correspond to genic regions; in particular, promoters and introns (Figure 7B). DOC1 appears to enhance promoter binding by NURD, which increased from ~23% to ~35% of all mapped binding sites (Figures 7B and 7C). Strikingly, DOC1 expression led to a substantially higher proportion of CHD4 binding at CpG islands (Figure 7D). Taken together, genome-wide binding analysis confirmed that DOC1 promotes NURD binding to a subset of target loci. In particular, our results support a role for DOC1 in NURD recruitment to CpG islands.

DISCUSSION

ATP-dependent chromatin remodelers are frequently mutated in human cancers. However, the molecular basis of the association between mutations in specific remodeler subunits and particular types of cancer is poorly understood. Here, we showed that the loss of DOC1 in oral cancer cells leads to a failure of NURD to bind and repress master transcriptional regulators of EMT. Re-expression of DOC1 in OSCC cells restores NURD recruitment to key target genes, a switch from open to closed chromatin, transcriptional repression, and reversal of EMT (MET). Consistent with the transcriptional repression we observed after DOC1-dependent NURD recruitment, the OSCC cells we studied harbor MBD2-NURD (Figure 1), the NURD variant implicated in the formation of repressive chromatin (Günther et al., 2013). In agreement with its effects in OSCC cells, depletion of DOC1 in HaCaT keratinocytes led to the induction of EMT, but also caused decreased cell proliferation (Figure 3). Moreover, knockdown of DOC1 in primary human fibroblasts induces p53-dependent cellular senescence (Alsayegh et al., 2015). Thus, in spite of its role as a tumor suppressor, loss of DOC1 normally blocks, rather than stimulates, cell proliferation. In all four of the OSCC cell lines we studied here, both the p53 and the INK4a tumor suppressor pathways have been compromised. We speculate that, during the development of oral cancer, DOC1 is lost after the inactivation of p53 and INK4a. The loss of DOC1 will then contribute to oncogenesis through transcriptional de-repression, EMT, and further loss of proliferation control. Our genome-wide binding site analysis showed that DOC1 is crucial for NURD recruitment to a subset of target loci. In particular, these experiments suggested a role for DOC1 in NURD binding to promoter regions harboring CpG islands. We did not investigate the effect of DNA methylation, but in vitro experiments suggested that DOC1 is not directly involved in recognition of methylated CpG residues (Spruijt et al., 2010). Alternatively, DOC1 may interact with specific sequence-selective transcription factors.

Our results revealed that, rather than working on a naive template, remodelers compete for access to chromatin. DOC1-mediated NURD binding to the *Twist1/2* and *Zeb2* promoters leads to eviction of SWI/SNF and a transition from active to repressive chromatin. This process involves nucleosome repositioning onto the NDR, histone deacetylation, recruitment of PRC2 and KDM1A with their associated histone modifications, and shutdown of transcription. Remarkably, all these effects of DOC1 expression could be mimicked by SWI/SNF depletion. In the absence of SWI/SNF, the NURD complex lacking DOC1 could bind the *Twist1/2* and *Zeb2* promoters. These observations suggest that these promoters are always targeted by a remodeler. Binding of either SWI/SNF or NURD determines opposite epigenetic states, thereby committing OSCC cells to either EMT or MET.

There are interesting parallels between our results in oral cancer cells and findings in other systems. In embryonic stem cells, SWI/SNF and NURD can have reverse effects on the nucleosome organization of shared targets (Hainer and Fazzio, 2015; Yildirim et al., 2011). Moreover, NURD has been implicated in

Figure 6. SWI/SNF Depletion Mimics the Effects of DOC1 Re-expression

(A) Depletion of SMARCA2 and SMARCA4 affects cell shape and actin organization. Indirect IF of SCC9 cells following either mock knockdown (KD) or KD of both SMARCA2 and SMARCA4. Cells were stained with antibodies against either SMARCA2 or SMARCA4 (red), F-actin was visualized by phalloidin staining (green). See Figure S5A for individual KDs.

(B) Immunoblotting analysis of the effect of SMARCA2/4 KD on EMT markers. See Figure S5B for individual KDs.

(C) Effect of SMARCA2/4 KD on the mRNA levels of *Twist1*, *Twist2*, and *Zeb2* and markers of EMT, as determined by qRT-PCR. Mock KD is indicated by yellow bars; SMARCA2/4 KD is indicated by red bars. *Gapdh* was used for normalization. Means and SDs were derived from three independent biological replicates. See Figures S5C and S5D for individual KDs and effects on cell numbers.

(D and E) ChIP-qPCR analysis of (D) SMARCA2 and (E) SMARCA4 binding to the Twist1/2 promoters following mock KD (yellow bars) or KD of both SMARCA2 and SMARCA4 (red bars). See Figure S6 for ChIP analysis of the *Zeb2* promoter.

(F) Loss of SMARCA2/4 leads to the occupation of the *Twist1* NDR. High-resolution MNase accessibility mapping after SMARCA2/4 KD. See the Figure 5C legend for details.

(G–J) ChIP-qPCR analysis of chromatin at the Twist1/2 promoters using antibodies directed against (G) CHD4, (H) H3K27ac, (I) EZH2 and (J) H3K27me3. Protein ChIP signals are presented as percentage of input chromatin. Histone modification ChIPs were normalized to H3 signals.

Means and SEMs for all experiments in this figure were derived from three independent biological replicates. Additional ChIP data are presented in Figure S5. Results for the *Zeb2* promoter are presented in Figure S6.

See also Figures S5 and S6.

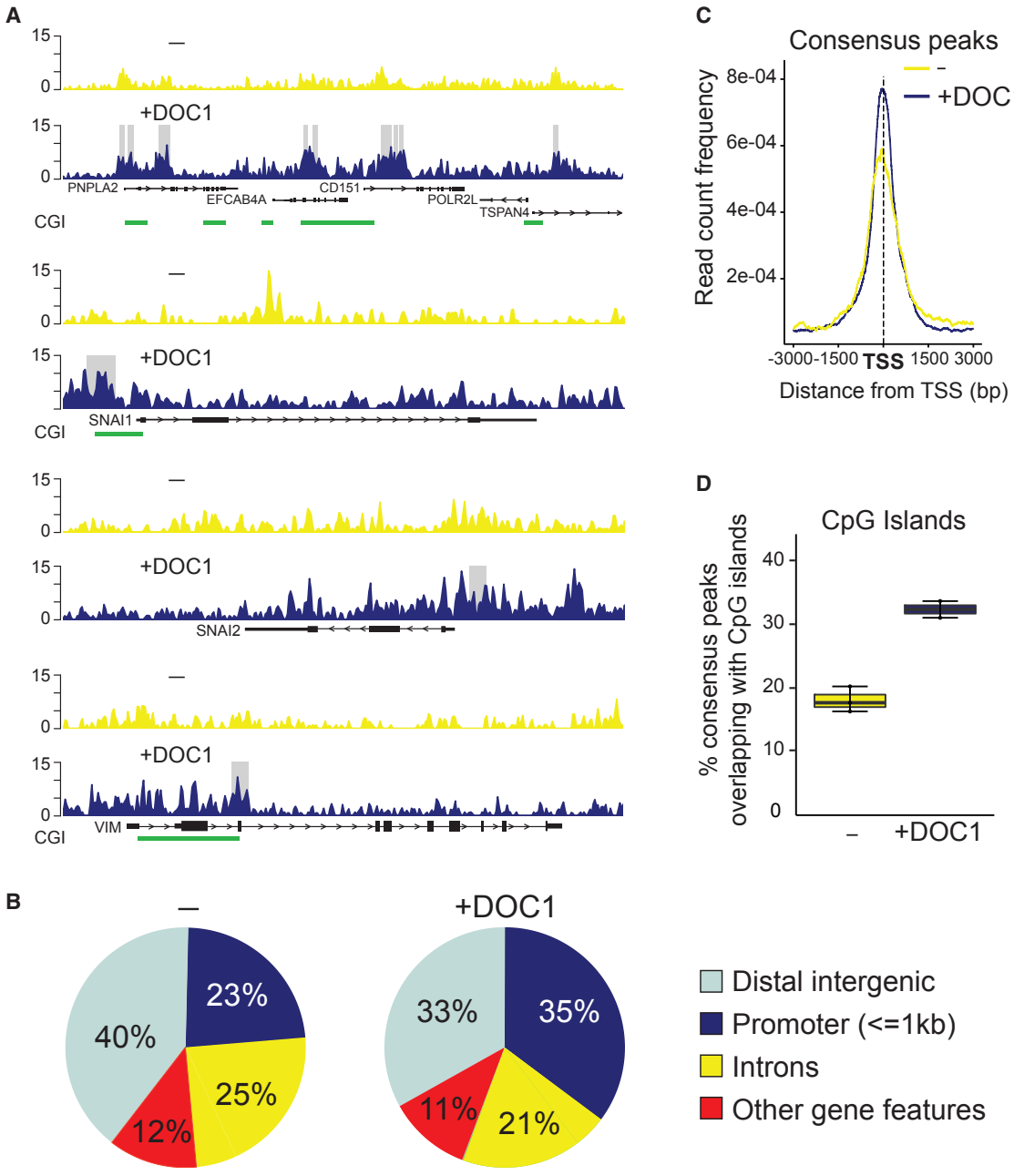

Figure 7. DOC1 Promotes NURD Binding to a Subset of Loci

(A) Genome browser track examples illustrating DOC1-dependent binding of CHD4 to CpG islands (CGI, green) and the *Snail* (*SNAI1*), *Slug* (*SNAI2*), and *Vimentin* genes. Read coverage of CHD4 ChIPs in the absence (yellow) or presence (blue) of DOC1. MACS2-called peaks are highlighted as gray bars.

(B) Distribution of CHD4 consensus peaks to their nearest genomic feature. CHD4 ChIP-seq on chromatin from SCC9 cells that either lack or express DOC1. Genomic features that corresponded to <4% of total peaks were aggregated into "other gene features," comprising: exons, 1–3 kb from promoter; 5′ UTR, ≤3 kb downstream; and 3′ UTR. Consensus peaks were derived from three (−DOC1) or two (+DOC1) biological replicates.

(C) Averaged CHD4 peak density (read count frequency) around the aligned transcription start sites (TSSs) of all known human genes (UCSC, hg19). −DOC1 is indicated in yellow, and +DOC1 is indicated in blue.

(D) Tukey-style boxplots representing the relative frequency of ChIP-seq peaks on human CpG islands.

Polycomb repression in flies and mice (Kehle et al., 1998; Morey et al., 2008; Reynolds et al., 2012; Sparmann et al., 2013). The link between NURD and Polycomb might involve a direct molecular mechanism, e.g., H3K27 deacetylation by NURD might promote PRC2 binding (Reynolds et al., 2012). Alternatively, transcriptional repression by NURD might allow the default binding

of PRC2 to CpG islands of silenced genes (Riising et al., 2014). Our results in OSCC cells emphasize the importance of the dynamic balance between NURD, Polycomb, and SWI/SNF function in human cancer.

It is instructive to compare the function of DOC1 in OSCCs with that of the SWI/SNF subunit SMARCB1/hSNF5 in malignant rhabdoid tumors (MRTs). MRTs are an extremely aggressive pediatric cancer caused by the loss of SMARCB1 (Masliah-Planchon et al., 2015; Wilson and Roberts, 2011). The absence of SMARCB1 precludes SWI/SNF binding to key tumor suppressor genes, leading to a failure to block Polycomb repression (Kia et al., 2008; Wilson et al., 2010). We showed previously that re-expression of SMARCB1 in MRT cells restores SWI/SNF recruitment, causing Polycomb eviction and activation of the *p16INK4a* and *p15INK4b* tumor suppressors (Kia et al., 2008). Thus, in contrast to NURD, SWI/SNF antagonizes Polycomb repression. Although the loss of DOC1 in OSCCs or that of SMARCB1 in MRTs generates opposite epigenetic states of their target genes, in both cases, this is caused by failed remodeler recruitment. The loss of a single subunit, such as DOC1 or SMARCB1, does not abrogate all other remodeler functions. For example, OSCC cells are still dependent on CHD4, MBD2, and MTA2 (Figures 3 and S3), and MRT cells require SMARCA4 for survival (Wang et al., 2009).

We suggest that subunit-dependent gene selection is a major cause of the association between the loss of specific remodeler subunits and particular types of cancer. Our results emphasize that gene control involves a dynamic equilibrium between opposing chromatin modulating enzymes rather than a static chromatin state. Disturbances in this balance can initiate a cascade of chromatin reprogramming events that drives oncogenesis. Such an intertwined system of epigenetic regulation suggests therapeutic strategies aimed at restoring the balance between antagonistic activities.

EXPERIMENTAL PROCEDURES

Cell-Based Assays

Tumor analysis and IF were performed using standard procedures. FLAG-tagged DOC1 was expressed using lentiviral transduction, followed by selection for expression of the lentiviral vector with blasticidin. DOC1-expressing cells were analyzed 2–10 days after transduction, but typically at day 4. shRNAs for knockdown experiments were delivered by lentiviral transduction, and cells were selected for blasticidin resistance and analyzed 4 days after transduction. For the wound-healing assay, cells were plated to confluence, and then a scratch was introduced with a pipette tip. Images were captured at 0 and 72 hr following scratching. Cell numbers were determined by using the Aqueous One Solution Cell Proliferation Assay (Promega). Means and SEMs were derived from three independent biological replicates. See the Supplemental Experimental Procedures for details, cloning, sequences, and antibodies used.

Biochemical Procedures

Most procedures were performed essentially as described previously (Chalkley and Verrijzer, 2004). WCEs were prepared by sonication in RIPA buffer (50 mM Tris [pH 7.5], 150 mM NaCl, 0.1% SDS v/v, 0.5% deoxycholate v/v, 1% NP-40 v/v, and protease inhibitors). Excess debris was removed by centrifugation. For IPs, WCEs prepared from $\sim 10^7$ cells were incubated with antibodies crosslinked to Protein A-Sepharose beads (Sigma), followed by sequential washes with HEMG/300 buffer (25 mM HEPES-KOH [pH 7.6], 0.1 mM EDTA, 12.5 mM $MgCl_2$, 10% glycerol, 0.1% NP-4, 300 mM KCl, and protease inhibitors), followed by washes with HEMG/600 mM NaCl, and finally HEMG/100 mm NaCl. Bound proteins were eluted by pH shock with glycine buffer (100 mM glycine, 150 mM NaCl [pH 2.5]). For mass spectrometric analyses, proteins were TCA (trichloroacetic acid) precipitated, resolved by SDS-PAGE, processed, and analyzed by nanoflow liquid chromatography-tandem mass spectrometry, as described previously (Moshkin et al., 2009). For co-IP-western blot experiments, cell extracts were incubated with antibodies cross-linked to Protein A-Sepharose beads. Beads were washed with HEMG/400 mM NaCl, HEMG/200 mM NaCl, and then bound proteins were dissolved in SDS loading buffer. Proteins were resolved by SDS-PAGE followed by immunoblotting. See the Supplemental Experimental Procedures for details and a list of antibodies used.

Chromatin Analysis and RNA Procedures

ChIP assays were performed using standard procedures. ChIP using species- and isotype-matched immunoglobulins were used to determine background levels. qPCR analyses were performed on immunoprecipitated DNA. The enrichment of specific DNA sequences was calculated by using the ΔCT method. All ChIP data presented are the result of at least three biological replicate experiments and triplicate qPCR reactions. Results were averaged, and SEs were determined. ChIPs against histone marks were normalized against histone H3. High-resolution MNase mapping was performed essentially as described previously (Sekinger et al., 2005; Rafati et al., 2011). For ChIP-seq, samples from three biological replicates were prepared according to the NEXTflex ChIP-Seq Kit (Bioo Scientific). ChIP libraries were sequenced according to the Illumina TruSeq Rapid v2 protocol on the HiSeq2500. Trimmed ChIP-seq reads were aligned to the human genome (hg19). Narrow peak calling was performed by MACS2, with a q-value cutoff of 0.01 using mock controls (−_IgG/+DOC1_IgG) per sample to reduce background noise and artifacts. One experiment (+DOC1, replicate #2) was removed from further analysis due to quality concerns. Consensus peak sets per condition (−DOC1, +DOC1) were generated using DiffBind (v2.2.8). Peaks were annotated using ChIPseeker (v1.10.3) and UCSC (University of California, Santa Cruz) hg19 annotations. For gene expression analysis, total RNA was isolated using the TriPure Isolation Reagent (Roche Diagnostics). RT was carried out on ~1 μg total RNA using SuperScript II RNase H Reverse Transcriptase (Invitrogen) and oligo(dT) or random hexamer primers. Real-time qPCR (MyIQ; Bio-Rad) was performed with the GoTaq qPCR Master Mix (Promega). *Gapdh* was used for normalization. See the Supplemental Experimental Procedures for details and a list of antibodies used.

ACCESSION NUMBERS

The accession number for the ChIP-seq data reported in this paper is GEO: GSE97839.

SUPPLEMENTAL INFORMATION

Supplemental Information includes Supplemental Experimental Procedures, six figures, and one table and can be found with this article online at http://dx.doi.org/10.1016/j.celrep.2017.06.020.

AUTHOR CONTRIBUTIONS

A.M.-S. and C.P.V. designed the research, analyzed the results, and wrote the manuscript, with input from all other authors. A.M.-S. performed all molecular and cellular assays. A.G.B. and D.Z. assisted with the IPs, IF, and cell culture. K.B. and J.A.D. performed the proteomic analysis. M.T., R.F., M.J.D.H., S.M.W., R.J.B.d.J., and L.H.J.L. were responsible for the oral cancer analysis. W.F.J.v.I. and E.O. performed next-generation sequencing. J.v.R. and H.J.G.v.d.W. performed analysis of ChIP-seq data.

ACKNOWLEDGMENTS

This work was supported in part by grants from The Netherlands Institute for Regenerative Medicine Consortium (FES0908) and the Netherlands Proteomics Centre to C.P.V.

Received: July 1, 2016
Revised: April 24, 2017
Accepted: June 4, 2017
Published: July 5, 2017

REFERENCES

Alsayegh, K.N., Gadepalli, V.S., Iyer, S., and Rao, R.R. (2015). Knockdown of CDK2AP1 in primary human fibroblasts induces p53 dependent senescence. PLoS ONE *10*, e0120782.

Becker, P.B., and Workman, J.L. (2013). Nucleosome remodeling and epigenetics. Cold Spring Harb. Perspect. Biol. *5*, a017905.

Chalkley, G.E., and Verrijzer, C.P. (2004). Immuno-depletion and purification strategies to study chromatin-remodeling factors in vitro. Methods Enzymol. *377*, 421–442.

Choi, M.G., Sohn, T.S., Park, S.B., Paik, Y.H., Noh, J.H., Kim, K.M., Park, C.K., and Kim, S. (2009). Decreased expression of p12 is associated with more advanced tumor invasion in human gastric cancer tissues. Eur. Surg. Res. *42*, 223–229.

dos Santos, R.L., Tosti, L., Radzisheuskaya, A., Caballero, I.M., Kaji, K., Hendrich, B., and Silva, J.C. (2014). MBD3/NuRD facilitates induction of pluripotency in a context-dependent manner. Cell Stem Cell *15*, 102–110.

Günther, K., Rust, M., Leers, J., Boettger, T., Scharfe, M., Jarek, M., Bartkuhn, M., and Renkawitz, R. (2013). Differential roles for MBD2 and MBD3 at methylated CpG islands, active promoters and binding to exon sequences. Nucleic Acids Res. *41*, 3010–3021.

Hainer, S.J., and Fazzio, T.G. (2015). Regulation of nucleosome architecture and factor binding revealed by nuclease footprinting of the ESC genome. Cell Rep. *13*, 61–69.

Hiyoshi, Y., Watanabe, M., Hirashima, K., Karashima, R., Sato, N., Imamura, Y., Nagai, Y., Yoshida, N., Toyama, E., Hayashi, N., and Baba, H. (2009). p12CDK2-AP1 is associated with tumor progression and a poor prognosis in esophageal squamous cell carcinoma. Oncol. Rep. *22*, 35–39.

Hu, G., and Wade, P.A. (2012). NuRD and pluripotency: a complex balancing act. Cell Stem Cell *10*, 497–503.

Kehle, J., Beuchle, D., Treuheit, S., Christen, B., Kennison, J.A., Bienz, M., and Müller, J. (1998). dMi-2, a Hunchback-interacting protein that functions in polycomb repression. Science *282*, 1897–1900.

Kia, S.K., Gorski, M.M., Giannakopoulos, S., and Verrijzer, C.P. (2008). SWI/SNF mediates polycomb eviction and epigenetic reprogramming of the INK4b-ARF-INK4a locus. Mol. Cell. Biol. *28*, 3457–3464.

Kim, Y., McBride, J., Kimlin, L., Pae, E.K., Deshpande, A., and Wong, D.T. (2009). Targeted inactivation of p12, CDK2 associating protein 1, leads to early embryonic lethality. PLoS ONE *4*, e4518.

Kolla, V., Naraparaju, K., Zhuang, T., Higashi, M., Kolla, S., Blobel, G.A., and Brodeur, G.M. (2015). The tumour suppressor CHD5 forms a NuRD-type chromatin remodelling complex. Biochem. J. *468*, 345–352.

Lai, A.Y., and Wade, P.A. (2011). Cancer biology and NuRD: a multifaceted chromatin remodelling complex. Nat. Rev. Cancer *11*, 588–596.

Laugesen, A., and Helin, K. (2014). Chromatin repressive complexes in stem cells, development, and cancer. Cell Stem Cell *14*, 735–751.

Luger, K., Mäder, A.W., Richmond, R.K., Sargent, D.F., and Richmond, T.J. (1997). Crystal structure of the nucleosome core particle at 2.8 A resolution. Nature *389*, 251–260.

Masliah-Planchon, J., Bièche, I., Guinebretière, J.M., Bourdeaut, F., and Delattre, O. (2015). SWI/SNF chromatin remodeling and human malignancies. Annu. Rev. Pathol. *10*, 145–171.

Menafra, R., and Stunnenberg, H.G. (2014). MBD2 and MBD3: elusive functions and mechanisms. Front. Genet. *5*, 428.

Morey, L., Brenner, C., Fazi, F., Villa, R., Gutierrez, A., Buschbeck, M., Nervi, C., Minucci, S., Fuks, F., and Di Croce, L. (2008). MBD3, a component of the NuRD complex, facilitates chromatin alteration and deposition of epigenetic marks. Mol. Cell. Biol. *28*, 5912–5923.

Morgan, M.A., and Shilatifard, A. (2015). Chromatin signatures of cancer. Genes Dev. *29*, 238–249.

Moshkin, Y.M., Kan, T.W., Goodfellow, H., Bezstarosti, K., Maeda, R.K., Pilyugin, M., Karch, F., Bray, S.J., Demmers, J.A., and Verrijzer, C.P. (2009). Histone chaperones ASF1 and NAP1 differentially modulate removal of active histone marks by LID-RPD3 complexes during NOTCH silencing. Mol. Cell *35*, 782–793.

Narlikar, G.J., Sundaramoorthy, R., and Owen-Hughes, T. (2013). Mechanisms and functions of ATP-dependent chromatin-remodeling enzymes. Cell *154*, 490–503.

Patel, D.J., and Wang, Z. (2013). Readout of epigenetic modifications. Annu. Rev. Biochem. *82*, 81–118.

Puisieux, A., Brabletz, T., and Caramel, J. (2014). Oncogenic roles of EMT-inducing transcription factors. Nat. Cell Biol. *16*, 488–494.

Rafati, H., Parra, M., Hakre, S., Moshkin, Y., Verdin, E., and Mahmoudi, T. (2011). Repressive LTR nucleosome positioning by the BAF complex is required for HIV latency. PLoS Biol. *9*, e1001206.

Reddy, B.A., Bajpe, P.K., Bassett, A., Moshkin, Y.M., Kozhevnikova, E., Bezstarosti, K., Demmers, J.A., Travers, A.A., and Verrijzer, C.P. (2010). *Drosophila* transcription factor Tramtrack69 binds MEP1 to recruit the chromatin remodeler NuRD. Mol. Cell. Biol. *30*, 5234–5244.

Reynolds, N., Salmon-Divon, M., Dvinge, H., Hynes-Allen, A., Balasooriya, G., Leaford, D., Behrens, A., Bertone, P., and Hendrich, B. (2012). NuRD-mediated deacetylation of H3K27 facilitates recruitment of Polycomb Repressive Complex 2 to direct gene repression. EMBO J. *31*, 593–605.

Riising, E.M., Comet, I., Leblanc, B., Wu, X., Johansen, J.V., and Helin, K. (2014). Gene silencing triggers polycomb repressive complex 2 recruitment to CpG islands genome wide. Mol. Cell *55*, 347–360.

Sekinger, E.A., Moqtaderi, Z., and Struhl, K. (2005). Intrinsic histone-DNA interactions and low nucleosome density are important for preferential accessibility of promoter regions in yeast. Mol. Cell *18*, 735–748.

Shintani, S., Ohyama, H., Zhang, X., McBride, J., Matsuo, K., Tsuji, T., Hu, M.G., Hu, G., Kohno, Y., Lerman, M., et al. (2000). p12(DOC-1) is a novel cyclin-dependent kinase 2-associated protein. Mol. Cell. Biol. *20*, 6300–6307.

Shintani, S., Mihara, M., Terakado, N., Nakahara, Y., Matsumura, T., Kohno, Y., Ohyama, H., McBride, J., Kent, R., Todd, R., et al. (2001). Reduction of p12DOC-1 expression is a negative prognostic indicator in patients with surgically resected oral squamous cell carcinoma. Clin. Cancer Res. *7*, 2776–2782.

Signolet, J., and Hendrich, B. (2015). The function of chromatin modifiers in lineage commitment and cell fate specification. FEBS J. *282*, 1692–1702.

Sparmann, A., Xie, Y., Verhoeven, E., Vermeulen, M., Lancini, C., Gargiulo, G., Hulsman, D., Mann, M., Knoblich, J.A., and van Lohuizen, M. (2013). The chromodomain helicase Chd4 is required for Polycomb-mediated inhibition of astroglial differentiation. EMBO J. *32*, 1598–1612.

Spruijt, C.G., Bartels, S.J., Brinkman, A.B., Tjeertes, J.V., Poser, I., Stunnenberg, H.G., and Vermeulen, M. (2010). CDK2AP1/DOC-1 is a bona fide subunit of the Mi-2/NuRD complex. Mol. Biosyst. *6*, 1700–1706.

Swygert, S.G., and Peterson, C.L. (2014). Chromatin dynamics: interplay between remodeling enzymes and histone modifications. Biochim. Biophys. Acta *1839*, 728–736.

Todd, R., McBride, J., Tsuji, T., Donoff, R.B., Nagai, M., Chou, M.Y., Chiang, T., and Wong, D.T. (1995). Deleted in oral cancer-1 (doc-1), a novel oral tumor suppressor gene. FASEB J. *9*, 1362–1370.

Torchy, M.P., Hamiche, A., and Klaholz, B.P. (2015). Structure and function insights into the NuRD chromatin remodeling complex. Cell. Mol. Life Sci. *72*, 2491–2507.

Wang, X., Sansam, C.G., Thom, C.S., Metzger, D., Evans, J.A., Nguyen, P.T., and Roberts, C.W. (2009). Oncogenesis caused by loss of the SNF5 tumor suppressor is dependent on activity of BRG1, the ATPase of the SWI/SNF chromatin remodeling complex. Cancer Res. *69*, 8094–8101.

Whyte, W.A., Bilodeau, S., Orlando, D.A., Hoke, H.A., Frampton, G.M., Foster, C.T., Cowley, S.M., and Young, R.A. (2012). Enhancer decommissioning by LSD1 during embryonic stem cell differentiation. Nature *482*, 221–225.

Wilson, B.G., and Roberts, C.W. (2011). SWI/SNF nucleosome remodellers and cancer. Nat. Rev. Cancer *11*, 481–492.

Wilson, B.G., Wang, X., Shen, X., McKenna, E.S., Lemieux, M.E., Cho, Y.J., Koellhoffer, E.C., Pomeroy, S.L., Orkin, S.H., and Roberts, C.W. (2010). Epigenetic antagonism between Polycomb and SWI/SNF complexes during oncogenic transformation. Cancer Cell *18*, 316–328.

Winter, J., Pantelis, A., Reich, R., Jepsen, S., Allam, J.P., Novak, N., and Wenghoefer, M. (2011). Risk estimation for a malignant transformation of oral lesions by S100A7 and Doc-1 gene expression. Cancer Invest. *29*, 478–484.

Wong, D.T., Kim, J.J., Khalid, O., Sun, H.H., and Kim, Y. (2012). Double edge: CDK2AP1 in cell-cycle regulation and epigenetic regulation. J. Dent. Res. *91*, 235–241.

Wu, L.C., Chen, Y.L., Wu, W.R., Li, C.F., Huang, H.Y., Lee, S.W., Chang, S.L., Lin, C.Y., Chen, Y.H., Hsu, H.P., et al. (2012). Expression of cyclin-dependent kinase 2-associated protein 1 confers an independent prognosticator in nasopharyngeal carcinoma: a cohort study. J. Clin. Pathol. *65*, 795–801.

Ye, X., and Weinberg, R.A. (2015). Epithelial-mesenchymal plasticity: a central regulator of cancer progression. Trends Cell Biol. *25*, 675–686.

Yildirim, O., Li, R., Hung, J.H., Chen, P.B., Dong, X., Ee, L.S., Weng, Z., Rando, O.J., and Fazzio, T.G. (2011). Mbd3/NURD complex regulates expression of 5-hydroxymethylcytosine marked genes in embryonic stem cells. Cell *147*, 1498–1510.

Zentner, G.E., and Henikoff, S. (2013). Regulation of nucleosome dynamics by histone modifications. Nat. Struct. Mol. Biol. *20*, 259–266.